

See discussions, stats, and author profiles for this publication at: <https://www.researchgate.net/publication/231675745>

Superstructures of Mesoscopic Monomolecular Sheets of Thiacyanine J Aggregates in Solution

ARTICLE *in* LANGMUIR · SEPTEMBER 2003

Impact Factor: 4.46 · DOI: 10.1021/la035013f

CITATIONS

16

READS

7

6 AUTHORS, INCLUDING:



Keisaku Kimura

Hosei University

186 PUBLICATIONS 3,732 CITATIONS

SEE PROFILE

Superstructures of Mesoscopic Monomolecular Sheets of Thiacyanine J Aggregates in Solution

Hiroshi Yao,* Yasushi Kagoshima, Shin-ichi Kitamura, Takeshi Isohashi, Yoshiki Ozawa, and Keisaku Kimura

Department of Material Science, Graduate School of Science, Himeji Institute of Technology, 3-2-1 Koto, Kamigori-cho, Ako-gun, Hyogo 678-1297, Japan

Received June 10, 2003. In Final Form: July 29, 2003

We have characterized superstructures of thiacyanine J aggregates in aqueous electrolyte solution in the dye concentration range between 2.5 and 80 mM. Fluorescence microscopy, polarized-light microscopy, and atomic force microscopy proved that the individual thiacyanine J aggregate possessed a mesoscopic rectangular sheetlike morphology ($\sim 3\text{--}7 \mu\text{m}$ wide and $\sim 10\text{--}30 \mu\text{m}$ long) consisting of a two-dimensional monomolecular layer of molecules. Synchrotron small-angle X-ray scattering revealed the superstructure of oriented monomolecular sheets which shows a disordered (nematic-like) or an ordered (smectic) layer alignment in solution. These superstructural behaviors can be interpreted in terms of the packing or alignments of the mesoscopic monomolecular sheets of the J aggregate as a function of the dye concentration.

Introduction

One of the well-known organic supramolecular assemblies caused by enthalpically driven attractive molecular interaction is the J aggregates.¹ J aggregates were discovered by Jelley and Scheibe^{2,3} and characterized by a narrow and intense absorption band that shows a bathochromic shift compared to the relevant monomer band.⁴ On the basis of such optical characteristics, the aggregates have been often used as photographic sensitizers.⁵ Moreover, the aggregates have become significant model systems to mimic light-harvesting complexes of photosynthetic bacteria.⁶ Recent interest has focused on the ability of J aggregates to exhibit coherent excitation phenomena which provide large optical nonlinearities.^{7–9} Therefore, there is great interest in understanding the relationships between the molecular alignment in aggregates and the spectroscopic properties such as the spectral line shape and peak energy. So far, many spectroscopic properties of J aggregates have been well-interpreted on the basis of one- or two-dimensional molecular assembly models such as the molecular exciton theory,^{10,11} extended-dipole model,¹² or transition density calculation.⁴

On the other hand, the detailed solution structures of J aggregates have remained the subject of some speculation and controversy probably due to the deficit of in situ measurements at the molecular level. Cryogenic transmission electron microscopy (cryo-TEM) is a useful method to clarify the aggregate structures and has revealed various morphologies of the J aggregate of pseudoisocyanine (PIC) or carbocyanine dye having dialkyl substituents;^{13–15} however, it cannot characterize the solution behaviors of the aggregate. Small-angle X-ray scattering (SAXS) can probe relatively large-scale in situ solution structures, which includes not only the diffraction of large lattice spacing of the order of 1–100 nm but also the scattering by perturbed or nonperiodic structures of mesomorphic materials.¹⁶ By using solution small-angle X-ray diffraction and NMR spectroscopy, Tiddy and co-workers have determined the superstructures of J aggregates of ionic cyanine dyes representing thiacyanine which form a liquid-crystalline phase in solution; however, the architectures of the aggregate have not been sufficiently determined due to the absence of the direct observation of the J aggregates.^{17,18}

Recently, we could directly visualize the mesoscopic morphologies and their transformation in supramolecular J aggregates of thiacyanine dye in solution with fluorescence microscopy and atomic force microscopy (AFM).^{19–21} Meanwhile, organization and formation of higher-order structures of such mesoscopic soft materials are becoming significant in a concentrated molecular system.^{22,23} Therefore, these studies and considerations gave us the motiva-

- * Corresponding author. E-mail: yao@sci.himeji-tech.ac.jp.
- (1) Möbius, D. *Adv. Mater.* **1995**, 7, 437.
- (2) Jelley, E. E. *Nature* **1936**, 138, 1009; **1937**, 139, 631.
- (3) Scheibe, G. *Angew. Chem.* **1936**, 49, 563; **1937**, 50, 212.
- (4) (a) Norland, K.; Ames, A.; Taylor, T. *Photogr. Sci. Eng.* **1970**, 14, 296. (b) Van der Auweraer, M.; Scheblykin, I. *Chem. Phys.* **2002**, 275, 285.
- (5) Herz, A. H. In *The Theory of the Photographic Process*, 4th ed.; James, T. H., Ed.; Macmillan: New York, 1977; Chapter 10.
- (6) McDermott, G.; Prince, S. M.; Freer, A. A.; Hawthornthwaite-Lawless, A. M.; Papiz, M. Z.; Cogdell, R. J.; Isaacs, N. W. *Nature* **1995**, 374, 517.
- (7) Hanamura, E. *Phys. Rev. B* **1988**, 37, 1273.
- (8) Spano, F. C.; Kuklinski, J. R.; Mukamel, S. *J. Chem. Phys.* **1991**, 94, 7534.
- (9) Knoester, J. *J. Chem. Phys.* **1993**, 99, 8466.
- (10) (a) Scherer, P. O. J.; Fisher, S. F. *Chem. Phys.* **1984**, 86, 269. (b) Spano, F. C.; Mukamel, S. *J. Chem. Phys.* **1989**, 91, 683. (c) Fidder, H.; Terpstra, J.; Wiersma, D. A. *J. Chem. Phys.* **1991**, 94, 6895. (d) Malyshev, V.; Moreno, P. *Phys. Rev. B* **1995**, 51, 14587. (e) Potma, E. O.; Wiersma, D. A. *J. Chem. Phys.* **1998**, 108, 4894.
- (11) Davydov, A. S. *Theory of Molecular Excitons*; Plenum Press: New York, 1971.
- (12) Czikkely, V.; Försterling, H. D.; Kuhn, H. *Chem. Phys. Lett.* **1970**, 6, 207.

- (13) von Berlepsch, H.; Böttcher, C.; Ouart, A.; Burger, C.; Dähne, S.; Kristein, S. *J. Phys. Chem. B* **2000**, 104, 5255.
- (14) von Berlepsch, H.; Böttcher, C.; Dähne, L. *J. Phys. Chem. B* **2000**, 104, 8792.
- (15) von Berlepsch, H.; Böttcher, C. *J. Phys. Chem. B* **2002**, 106, 3146.
- (16) Chu, B.; Hsiao, B. S. *Chem. Rev.* **2001**, 101, 1727.
- (17) Harrison, W.; Mateer, D. L.; Tiddy, G. J. T. *J. Phys. Chem.* **1996**, 100, 2310.
- (18) Harrison, W. J.; Mateer, D. L.; Tiddy, G. J. T. *Faraday Discuss.* **1996**, 104, 139.
- (19) Yao, H.; Kimura, K. *Chem. Phys. Lett.* **2001**, 340, 211.
- (20) Yao, H.; Kitamura, S.; Kimura, K. *Phys. Chem. Chem. Phys.* **2001**, 3, 4560.
- (21) Yao, H.; Omizo, M.; Kitamura, N. *Chem. Commun.* **2000**, 739.
- (22) Vranken, N.; Fouquet, P.; Köhn, F.; Gronheid, R.; Scheblykin, I.; Van der Auweraer, M.; De Schryver, F. C. *Langmuir* **2002**, 18, 8407.

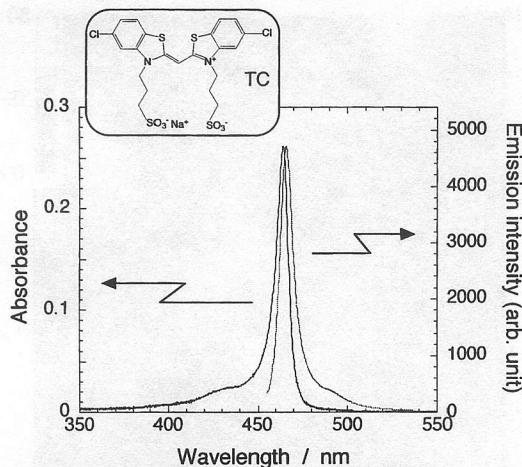


Figure 1. Absorption and fluorescence spectra of TC J aggregates (2.5 mM) in aqueous NaCl solution. The concentration of NaCl is 11 mM.

tion to investigate once more the detailed superstructures of the thiacyanine J aggregate in solution using synchrotron SAXS along with various microscopic techniques such as fluorescence microscopy, polarized-light microscopy, and AFM. In this article, we report a systematic study on the formation of superstructures of thiacyanine J aggregates in aqueous solutions. The mesoscopic rectangular sheet morphology of J aggregates was clarified, consisting of a two-dimensional monomolecular layer of dye molecules. We also found that orientation of the monomolecular sheets of the J aggregate caused the formation of disordered or ordered layer superstructures in concentrated dye solutions.

Experimental Section

Chemicals. The thiacyanine (TC) dye, 5,5'-dichloro-3,3'-disulfonylpropyl thiacyanine sodium salt (the chemical structure is shown in the inset in Figure 1), was purchased from Hayashibara Kankoh-Shikiso Kenkyusho and used as received. Sodium chloride (NaCl, GR grade) was purchased from Wako Pure Chemicals and used without further purification. Pure water was obtained by using an Aquarius GSR-200 (Advantec Co.) water distillation system. Sample solutions were prepared as follows: TC was dissolved in an aqueous NaCl solution ($[NaCl] = 11$ mM) under gentle heating; then, the solution was cooled with ice-water for about 1 h and left for several days at room temperature for equilibration.²⁴ The concentration of TC was changed between 2.5 and 80 mM.

Methods. (a) *Spectroscopy.* Absorption spectra were recorded with a Hitachi U-4100 spectrophotometer, and fluorescence spectra with a Hitachi F-4500 spectrofluorometer. Samples were contained between glass microscope slides and coverslips to form very thin solution films.

(b) *Microscopy.* Fluorescence micrographs were obtained by using a CCD camera (Flovle; HCC-600) set on an optical microscope (Olympus; BX-60). The excitation source (435 nm) was obtained by passing the light from an Hg lamp through a mirror cube unit (U-MNBV). Polarized-light microscopy (orthoscopy) was performed with an optical microscope (Nikon; Optiphot-pol) with crossed polarizers. The solution samples were contained between glass slides and coverslips. AFM topographical images were recorded with a Nanoscope IIIa system (Digital Instruments) operating in the tapping or contact mode. Microcantilevers made of Si (Digital Instruments; NCH; spring constant, 30–40 N m⁻¹) or Si₃N₄ (Digital Instruments; NP-S; spring constant, 0.12 N m⁻¹) were used for tapping or contact mode operation, respectively. Samples for the AFM measurements were prepared by placing an aliquot of TC solution on the freshly cleaved mica.

(23) Hamley, I. W. *Introduction to Soft Matter: Polymers, Colloids, Amphiphiles and Liquid Crystals*; John Wiley & Sons: Chichester, 2000.

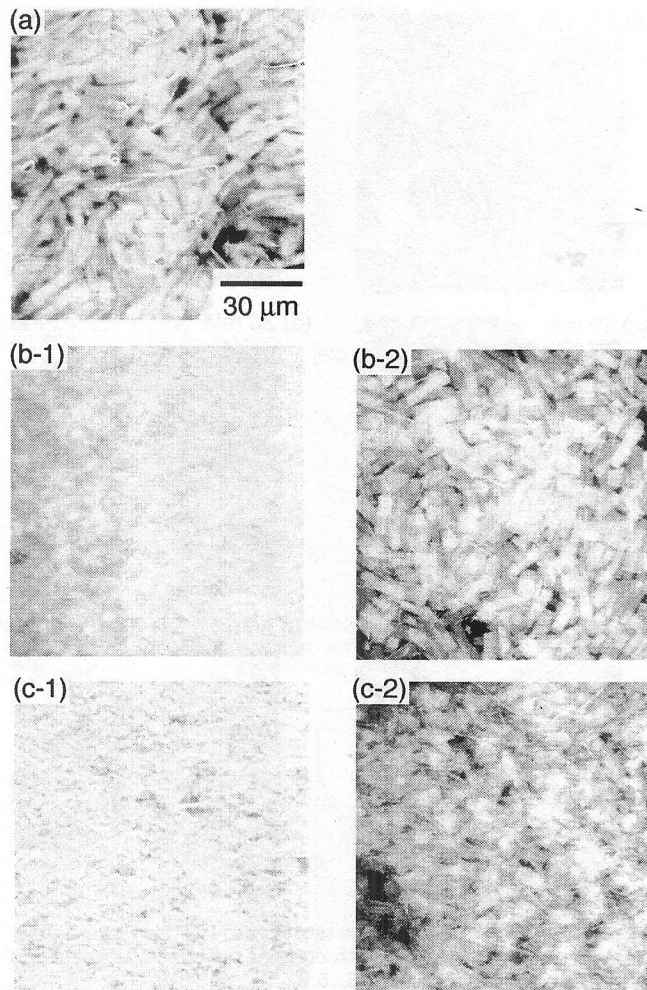


Figure 2. Fluorescence micrographs of the TC J aggregates in aqueous NaCl solution. Panels a, b-1, and c-1 show images at $[TC] = 2.5, 5.0$, and 10 mM, respectively. Panels b-2 and c-2 show images at $[TC] = 5.0$ and 10 mM, respectively, after photobleaching by photoirradiation of the samples with an excitation beam under the microscope. J aggregates possessing a mesoscopic rectangular sheetlike morphology can be seen.

(c) *Small-Angle X-ray Scattering (SAXS).* SAXS measurements were carried out using the BL40B2 beamline at the SPring-8 in Hyogo (Japan). This beamline provides the white X-rays generated by a bending magnet (magnetic field, 0.679 T). The beam was monochromatized (wavelength, $\lambda = 0.1196$ nm) and collimated with a quadrant slit in the beamline optics, and excess scattering was removed by three quadrant slits. The scattering patterns were recorded using an imaging plate area detector (300 × 300 mm; Rigaku; R-AXIS IV++) with a sample-to-detector distance of 1.0 m. The usable span of scattering vector magnitudes q ($q = 4\pi \sin(\theta)/\lambda$, where 2θ is the scattering angle) was in the range of 0.10 – 7.8 nm⁻¹. The aqueous dye samples (2.5–30 mM) were contained in a quartz cell (path, 1.0 mm). The scattering intensities were corrected for background scattering from the empty cell under the same optics. The sample solution of 80 mM was placed onto a Kapton film for the SAXS measurement because this solution was too viscous to be contained in the cell. For this sample, the scattering intensity was corrected for background arising from the same Kapton film. All experiments were carried out at room temperature.

Results and Discussion

Microscopic Characterization. Figure 1 shows the typical absorption and fluorescence spectra of an aqueous

(24) An aqueous NaCl solution was used to prepare the dye solutions only for promoting J aggregation based on our previous studies (ref 20).

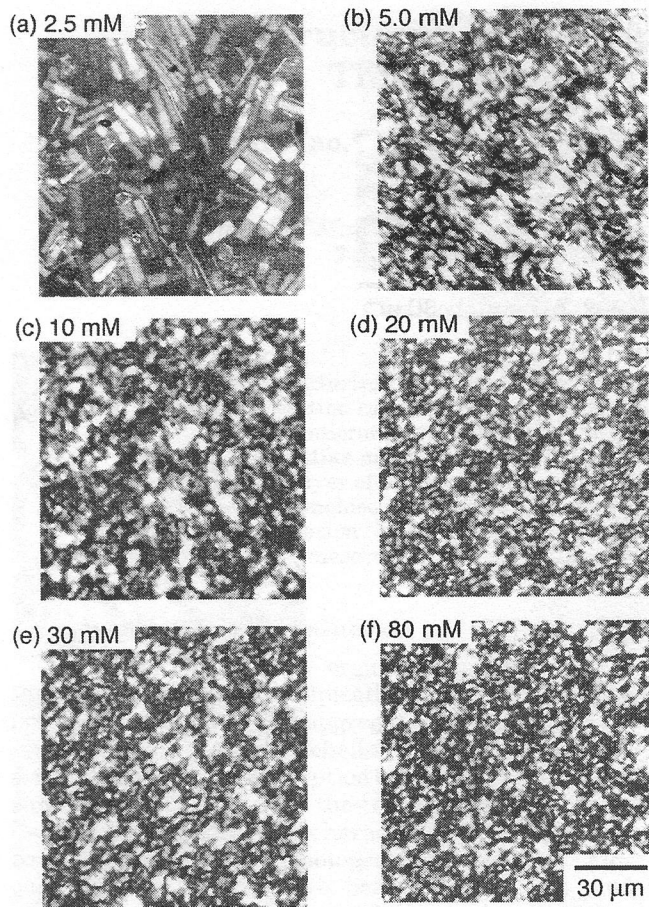


Figure 3. Optical microscope textures of the TC J aggregates in aqueous NaCl solution with crossed polarizers. Panels a–f show images at $[TC] = 2.5, 5.0, 10, 20, 30$, and 80 mM , respectively.

TC solution ($[TC] = 2.5\text{ mM}$). The absorption spectrum showed a sharp and intense J band at $\sim 464\text{ nm}$.²⁰ Note that a large increase in dye concentration and/or a long optical path length produced broadening of the J band (see ref 19). This broadening is caused not by a change in the internal structure of the J aggregates but by the reduction of the apparent absorption cross section due to the densely dispersed aggregate particles.¹⁹ The observed fluorescence spectrum does not show a Stokes shift, which is characteristic of the J aggregate.

Fluorescence microscopy was applied to determine the in situ microstructures of the TC J aggregates, because our previous studies proved that the aggregates possessed exclusively mesoscopic morphology with a highly emissive property resulting in formation of a distinctive opalescence of the solution.^{20,21} Figure 2a shows a typical fluorescence micrograph of the J aggregate at $[TC] = 2.5\text{ mM}$, clearly showing a mesoscopic rectangular sheetlike morphology as an overwhelming component. When the TC concentration was increased, the obtained microscope images became too bright to clarify the morphology of each aggregate, implying that fluorescence microscopy might be ineffective for the observation at high dye concentrations. Panel b-1 or panel c-1 of Figure 2 shows a typical fluorescence micrograph at $[TC] = 5.0$ or 10 mM , respectively, which shows a very obscure image. However, upon irradiation of the excitation beam to the sample under the microscope, the sheetlike morphology similar to that observed at $[TC] = 2.5\text{ mM}$ has appeared (panel b-2 or panel c-2 of Figure 2). The appearance of clear images is attributed to a decrease in the number of J aggregate

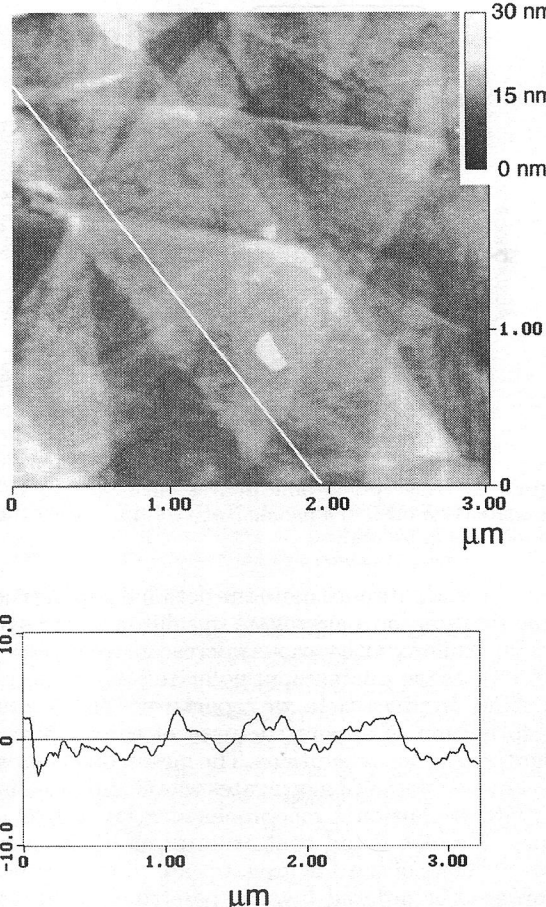


Figure 4. AFM topographical image of the sheetlike J aggregates on mica. The cross-sectional profile along the white line is also shown.

sheets due to photobleaching. The results indicate that the morphology of the J aggregate did not change with the increase in the TC concentration ($\geq 2.5\text{ mM}$). Therefore, it is reasonable to consider that the TC J aggregate possesses a sheetlike morphology at above 2.5 mM TC. The short-axis or long-axis length of the rectangular sheets was $\sim 3\text{--}7$ or $\sim 10\text{--}30\text{ }\mu\text{m}$, respectively.

If the sheet is composed of regularly aligned assemblies of TC molecules, observation of birefringence can be expected. Figure 3a shows a typical polarized-light microscope image with crossed polarizers at $[TC] = 2.5\text{ mM}$. The bright image clearly showed a rectangular sheetlike morphology of the J aggregate with strong birefringence. The size of the sheet was $\sim 10\text{--}25\text{ }\mu\text{m}$ in length and $\sim 4\text{--}8\text{ }\mu\text{m}$ in width, indicating that the morphology observed by using polarized-light microscopy corresponds to that by fluorescence microscopy. The sheet showed a straight extinction; namely, a dark image was obtained when the long axis of the sheet was parallel to the direction of polarization of the analyzer. This property indicates that the sheetlike aggregates possess a uniaxial lattice alignment of molecules. At $[TC] = 5.0\text{ mM}$, a polarized-light microscope image with crossed polarizers (Figure 3b) showed a disturbed rectangular morphology. When the dye concentration was further increased ($\geq 10\text{ mM}$), the micrographs exhibited vague grainy birefringent textures bearing little resemblance to those of other lyotropic mesophases.²³ Typical micrographs with crossed polarizers at $[TC] = 10\text{--}80\text{ mM}$ are shown in Figure 3c–f, respectively. These images are quite similar to each other, indicating that the intrinsic morphology (namely, sheetlike morphology) of the aggregates does not change. The

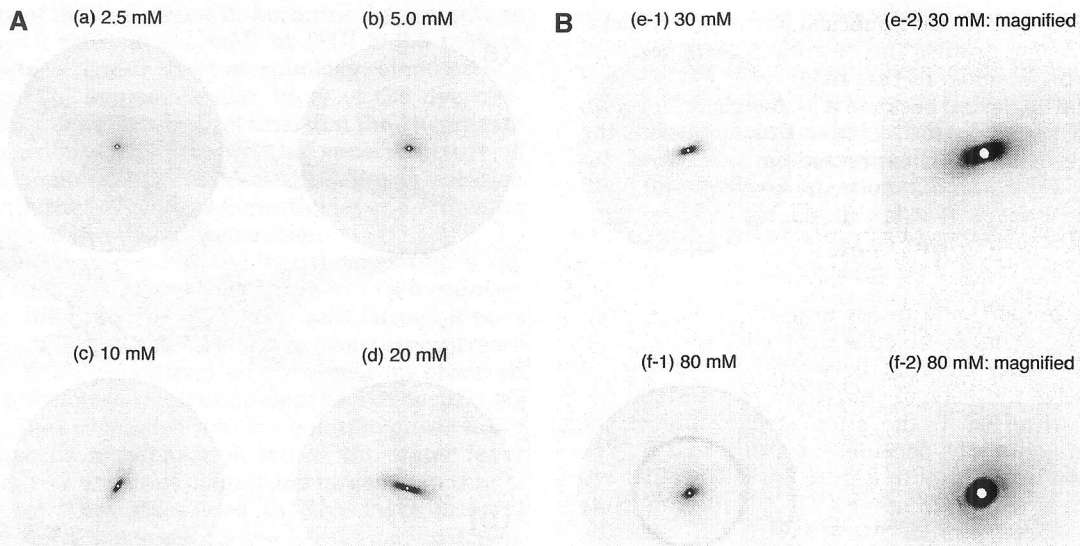


Figure 5. 2D SAXS patterns of the sample solutions of the TC J aggregates. Panels a–f show images at $[TC] = 2.5, 5.0, 10, 20, 30$, and 80 mM , respectively. Panels e-2 and f-2 show magnified patterns at the vicinity of the center. The sample-to-detector distance is 1.0 m .

observed microscopic textures are ascribed to stacking of the birefringent sheets in solution, and it might be impossible to distinguish the phase as is frequently determined for liquid crystals.

To clarify the thickness of the sheetlike aggregates, AFM measurements were conducted at ambient conditions. We prepared a sample in which a drop of solution was dried on a mica substrate. Before the AFM measurements, we confirmed that a similar fluorescence microscope image to that in solution was obtained. Figure 4 shows a typical AFM image and cross-sectional profile along the line in the image ($[TC] = 2.5\text{ mM}$). Although the J aggregate sheets are piled onto each other, careful analysis of the cross-sectional profile shows that the single sheets were $\sim 2\text{ nm}$ high, indicating a monomolecular layer structure. (Note that a TC molecule possesses a π -electron chromophore of about 0.5 nm and sulfopropyl groups of about 0.6 nm . For symmetry reasons, the dye molecules are presumably arranged within the layers with their sulfopropyl groups distributed above and below the layer plane, providing the effective layer thickness of about 1.7 nm .¹⁴) In conclusion, the free-standing sheetlike J aggregate consists of a two-dimensional monomolecular layer of TC molecules.²⁵

SAXS Analysis. To investigate the distribution properties (superstructures) of the J aggregate monomolecular sheets in solution, synchrotron SAXS studies were carried out at the SPring-8. Figure 5 shows typical two-dimensional (2D) SAXS patterns of TC solutions at different dye concentrations ($2.5\text{--}80\text{ mM}$). The scattering pattern was almost isotropic (azimuth independent) at $[TC] \leq 5.0\text{ mM}$, whereas it became anisotropic at $[TC] \geq 10.0\text{ mM}$. Note that the diffraction ring observed around the middle of the imaging plate ($q \sim 4.0\text{ nm}^{-1}$) is ascribed to the X-ray beam windows made of Kapton films.

Figure 6a shows the $\ln[I(q)]$ versus q^2 plot (Guinier plot) at $[TC] = 2.5$ or 5.0 mM extracted from panel a or panel b of Figure 5, respectively. Both profiles are quite similar and show a remarkable nonlinear behavior.²³ The non-

(25) A similar sheetlike morphology of the J aggregates was observed at $[TC] > \sim 5\text{ mM}$ in the absence of NaCl. We believe that NaCl does not affect the characteristic sheetlike morphology of TC J aggregates at a relatively high dye concentration.

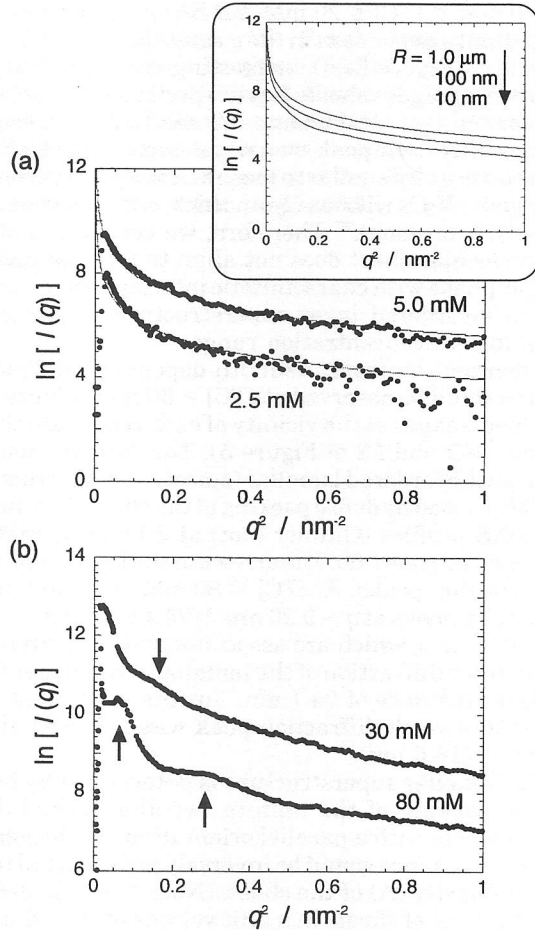


Figure 6. SAXS profiles (Guinier plot) of the sample solutions of the TC J aggregates. (a) $[TC] = 2.5$ and 5.0 mM . Simulated curves based on the flat disk dispersion model are also shown. The inset shows the simulated scattering profiles at $R = 10\text{ nm}$, 100 nm , and $1.0\text{ }\mu\text{m}$. (b) $[TC] = 30$ and 80 mM . The diffraction peaks ascribed to a smectic phase are indicated by arrows in the figure.

linearity is considered to arise from the scattering from the individual mesoscopic sheets of the J aggregate,

different from that from the spherical particle.^{23,26} Therefore, the scattering profiles can be simulated by a model for flat disk dispersions. In this model, the thickness of the disk can be neglected because it is much smaller than the radius of the disk (R).²⁶ Under this condition, the scattering intensity $I(q)$ is expressed as

$$I(q) = I_0 \frac{2}{q^2 R^2} \left(1 - \frac{1}{qR} J_1(2qR) \right) \quad (1)$$

where I_0 is a proportional factor and $J_1(2qR)$ is a first-order Bessel function. I_0 includes the contributions from the electron density contrast between the particles (J aggregates) and the solvent and from the volume per particle. By using eq 1, the simulated profile of the scattering intensity was obtained at a different R . The result is shown in the inset in Figure 6a. The profiles are almost identical with each other at $R \geq \sim 100$ nm. Note that the measured profiles were well fitted with the simulation curves at $R \geq \sim 100$ nm. (The solid curves in Figure 6a represent the simulated ones at $R = 1.0 \mu\text{m}$.) These results indicate that the isotropic SAXS profiles obtained at $[\text{TC}] = 2.5$ or 5.0 mM reflect the scattering from randomly distributed mesoscopic sheets of the J aggregate in solution.

At $10 \text{ mM} \leq [\text{TC}] \leq 20 \text{ mM}$, 2D SAXS diffuse patterns were azimuth dependent in the q range between ~ 0.1 and $\sim 1.0 \text{ nm}^{-1}$ (Figure 5c,d), suggesting that the monomolecular J aggregate sheets have a preferable orientation with face-to-face alignments in solution; however, a distinct diffraction peak was not detected. These SAXS patterns were also similar to those of a nematic suspension of inorganic V_2O_5 ribbons (1 nm thick, ~ 25 nm wide, and ~ 200 – 600 nm long).²⁷ Therefore, we conclude that the monomolecular sheet does not align to form an ordered lamellar phase with characteristic interlayer distance but forms a disordered layer superstructure (nematic-like phase) in that concentration range.

In marked contrast, azimuth-dependent diffraction patterns could be observed at $[\text{TC}] \geq 30 \text{ mM}$ (Figure 5e,f; magnified images at the vicinity of each center are shown in panels e-2 and f-2 of Figure 5). The results show the appearance of ordered lamellar (smectic) superstructures probably caused by dense packing of the sheets in solution. The SAXS profiles (Guinier plot) at 30 and 80 mM are also shown in Figure 6b. The arrows in the figure represent the diffraction peaks. At $[\text{TC}] = 80 \text{ mM}$, we could detect two distinct peaks at $q \sim 0.26 \text{ nm}^{-1}$ (24.1 nm) and $q \sim 0.53 \text{ nm}^{-1}$ (12.0 nm), which are associated with the first- and second-order diffraction of the lamellar structure with an interlayer distance of 24.1 nm. For the solution at $[\text{TC}] = 30 \text{ mM}$, a weak diffraction peak was observed at $q \sim 0.38 \text{ nm}^{-1}$ (16.6 nm).

If the lamellar superstructure is determined by homogeneous packing of the infinite two-dimensional J aggregate sheets with a parallel orientation in solution, the interlayer distance would be inversely proportional to the number density (Λ) of the sheet. (Note that Λ is defined as the number of sheets in a unit volume of the solution.) However, the J aggregate sheet is not infinite in size. Therefore, the interlayer distance is expected to show an inverse dependence on $\Lambda^{1/3}$. Considering that the dye concentration would be linearly correlated to Λ , we could estimate the interlayer distance to be 33.4 nm at $[\text{TC}] = 30 \text{ mM}$. Then, the observed peak at $q \sim 0.38 \text{ nm}^{-1}$ (16.6 nm) appropriately corresponds to the second-order dif-

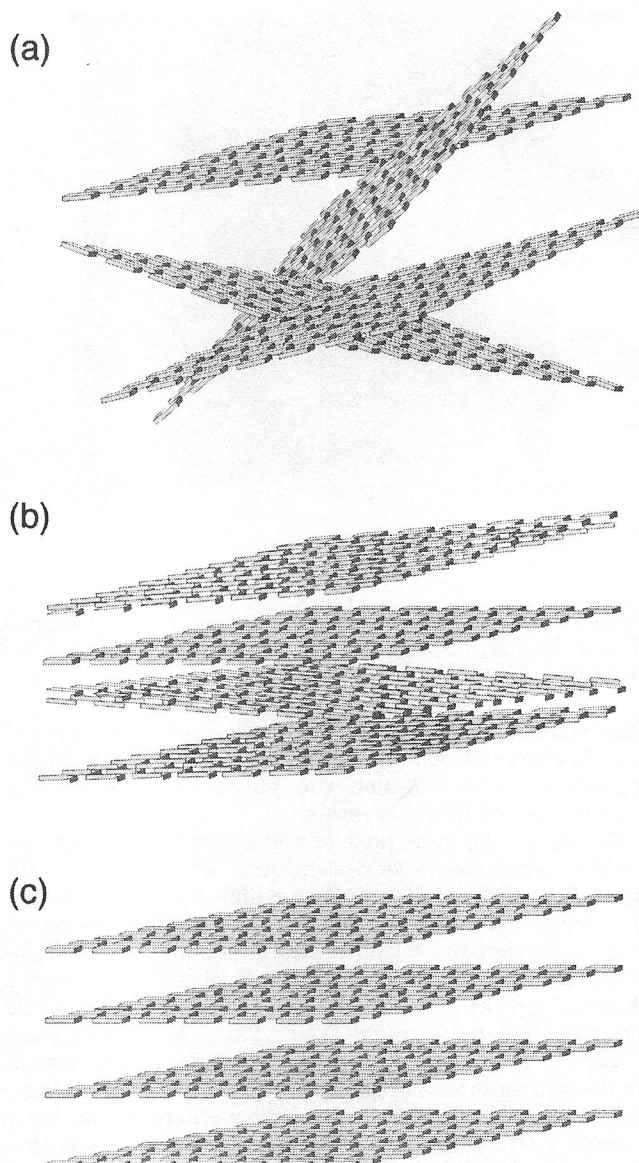


Figure 7. Schematic representation of the superstructures of the J aggregate monomolecular sheets in solution at different dye concentrations. The TC dye molecule is considered as a rigid box in this scheme. Panels a–c show the randomly distributed, disordered (nematic-like), and ordered (smectic) layer phases, respectively.

fraction of the lamellar structure. Because we could not observe any higher order (\geq third) diffraction even at $[\text{TC}] = 80 \text{ mM}$, the diffraction order assignment and the obtained interlayer distance at 30 mM are reasonable.²⁸ We conclude that the interlayer distance in the lamellar structures is dependent on the J aggregate sheet number density (or dye concentration): the higher the $[\text{TC}]$, the shorter the interlayer distance. This indicates that the lamellar alignment is probably driven by interaggregate steric interaction and stabilized by electrostatic repulsive interactions between negatively charged J aggregate sheets with sulfonate moieties.

Superstructures of the Monomolecular Sheets of J Aggregates in Solution.

We have revealed the rigid

(26) Kratky, O.; Porod, G. *J. Colloid Sci.* **1949**, *4*, 36.

(27) Gabriel, J.-C. P.; Davidson, P. *Adv. Mater.* **2000**, *12*, 9.

(28) If interlayer distance was inversely proportional to Λ (or dye concentration), we could calculate the characteristic distance to be 62.3 nm. The result is inappropriate because the observed peak at $q \sim 0.38 \text{ nm}^{-1}$ (16.6 nm) corresponds to neither the third-order (20.8 nm) nor the fourth-order (15.6 nm) diffraction of the lamellar structure.

morphology of the individual thiacyanine J aggregate in aqueous NaCl solution (11 mM) at $[TC] \geq 2.5$ mM: a mesoscopic rectangular sheet morphology composed of a two-dimensional monomolecular layer of the dye molecules. We also found for the first time that the J aggregate sheets are oriented to produce the superstructure of disordered (nematic-like) layer alignments in solution together with that of ordered (smectic) layer alignments as a function of the dye concentration.

Tiddy and co-workers showed by using solution X-ray diffraction that a similar thiacyanine dye (the counter-cation was different from that we used) formed a pure lamellar phase of the J aggregates in aqueous concentrated solutions.¹⁷ Since the diffraction patterns they observed appeared to exhibit concentration-dependent sharp Bragg reflections, they concluded that the solution phase was a swelling smectic mesophase in which the water layer thickness is 1–2 orders of magnitude larger than that of the dye layer. They calculated the dye layer to be of monomolecular thickness from the X-ray spacing dependence on the dye volume fractions by assuming that the aggregates are flat and infinite.^{17,18} In the present study, we could observe a similar lamellar phase of J aggregates in electrolyte solutions only at a relatively high dye concentration (≥ 30 mM), although some experimental conditions were different from their system.²⁹ A disordered layer structure (nematic-like phase) could also be recognized for the first time on the basis of our diffuse anisotropic SAXS patterns at a relatively low dye concentration. The disordered layer structure comes from the finite size of the J aggregate sheet. It should be emphasized that these superstructural behaviors of the J aggregate

(29) Despite some differences in the experimental conditions, our results (observation of lamellar structures of the J aggregates) obtained at $[TC] \geq 30$ mM are qualitatively consistent with those obtained by Tiddy and co-workers.

in solution can be reasonably interpreted in terms of the concentration-dependent packing or alignments of the mesoscopic monomolecular sheets of the aggregate, which could be directly visualized and characterized *in situ*.

Our conclusion on the solution J aggregate behaviors of the TC dye is schematically summarized in Figure 7. At a low dye concentration ($2.5 \text{ mM} \leq [TC] \leq 5 \text{ mM}$), the aggregate monomolecular sheet was randomly distributed in solution (Figure 7a) as revealed by SAXS measurements. We could distinguish the individual mesoscopic rectangular J aggregate sheet by using a fluorescence and/or a polarized-light microscope. In an intermediate dye concentration range ($10 \text{ mM} \leq [TC] \leq 20 \text{ mM}$), anisotropic diffuse SAXS patterns elucidated that the aggregate sheets were oriented to form a disordered layer structure (Figure 7b). At a high dye concentration (≥ 30 mM), the monomolecular sheets were oriented to produce an ordered layer (lamellar) phase with characteristic interlayer distance (Figure 7c). For steric reasons, the interlayer distance was dependent on the sheet number density (or dye concentration); the higher the TC concentration, the shorter the interlayer distance. Further studies include the detailed examination of electrolyte effects on the organization of mesoscopic soft materials consisting of various J aggregate morphologies.

Acknowledgment. We thank Japan Synchrotron Radiation Research Institute (JASRI) for the allocation of beam time at the SPring-8, Hyogo (Japan). We are also grateful to Drs. Keiko Miura and Katsuaki Inoue (JASRI) for their technical assistance in SAXS measurements. Financial support in part by the Hyogo Science and Technology Association is gratefully acknowledged.

LA035013F